Polymorphism in the Germanides *RE*PdGe with the Heavy Rare Earth Elements

Ute Ch. Rodewald, Birgit Heying, Rolf-Dieter Hoffmann, Dirk Niepmann, and Rainer Pöttgen

Institut für Anorganische und Analytische Chemie, Universität Münster, Corrensstraße 30, D-48149 Münster, Germany

Reprint requests to R. Pöttgen. E-mail: pottgen@uni-muenster.de

Z. Naturforsch. **2009**, *64b,* 595 – 602; received January 7, 2009

Dedicated to Professor Gerhard Maas on the occasion of his 60th birthday

The structures of the equiatomic germanides *RE*PdGe with the heavy rare earth elements have been reinvestigated with respect to palladium-germanium ordering. The samples were prepared by arc-melting of the elements followed by annealing procedures in sealed silica ampoules at different temperatures. The structures of YPdGe, HT-TbPdGe, LT-DyPdGe, HT-DyPdGe, LT-HoPdGe, HT-HoPdGe, ErPdGe, and TmPdGe, and of the new germanide LuPdGe, were refined from single crystal diffractometer data. LT-DyPdGe and LT-HoPdGe crystallize with the YPdSi-type structure, space group *Pmmn*. The other germanides crystallize with the non-centrosymmetric YbAuSn structure, space group *Imm2*. All structures are orthorhombically-distorted superstructure variants of AlB_2, and they show strong intralayer Pd–Ge bonding within the ordered Pd_3Ge_3 hexagons. There is weak Pd–Ge and Pd–Pd interlayer bonding. The crystal chemical relationship between the different superstructures is discussed.

Key words: Intermetallics, Rare Earth, Germanides, Crystal Chemistry, Superstructure

Introduction

The equiatomic germanides *RE*PdGe (*RE* = rare earth element) have repeatedly been studied in the last thirty years with respect to their crystal chemistry and physical properties [1 – 24]. An overview on the work on the *RE*PdGe germanides with the light rare earth elements is given in [21]. In the original work [1], these germanides have been assigned the KHg_2 ($CeCu_2$) type structure [25, 26], space group *Imma*, with statistical distribution of the palladium and germanium atoms on the mercury sites. Recent single crystal investigations on *RE*PdGe with *RE* = La, Ce, Pr, Nd, Sm, Gd, and Tb [21] and on YbPdGe [24], however, revealed full ordering of these atoms and superstructure formation with doubling or tripling of the subcells. All of these ordering variants belong to the orthorhombic branch of the many AlB_2-related superstructures [27].

So far, the superstructures TiNiSi (simple cell, *Pnma*) [28], CaCuGe (tripled cell, *Pnma*) [29, 30], CaAuSn (quintupled cell, *Pnma*) [30], YPdSi (doubled cell, *Pmmn*) [31], EuAuGe (simple cell, *Imm*2) [32], EuAuSn (quintupled cell, *Imm*2) [33], and YbAuSn (tripled cell, *Imm*2) [34] of the KHg_2 type are known. Since these superstructure variants have primitive or body-centered Bravais lattices, this is a good prerequisite for the structure assignment. If the cell enlargement (simple, doubled, tripled, or quintupled cell) and the Bravais lattice are known, then the assigment of the superstructure type is clear. Nevertheless, difficulties can arise if the orthorhombic distortion (ingoing from the AlB_2 subcell) is small (close to $\sqrt{3}$) or if the crystals reveal twinning.

So far, the Pd/Ge ordering had only been determined for the orthorhombic *RE*PdGe germanides with *RE* = La, Ce, Pr, Nd, Sm, Gd, and Tb [21], and very recently for YbPdGe [24] on high-quality crystals grown by the Bridgman technique. In the course of our systematic studies on AlB_2-related superstructures [27] we have extended our investigations on the precise palladium / germanium ordering with respect to the *RE*PdGe phases with the smaller rare earth elements. Herein we report on the polymorphism in TbPdGe, DyPdGe, and HoPdGe, the structure refinements of YPdGe, ErPdGe, and TmPdGe, and on the new germanide LuPdGe.

Table 1. Lattice parameters of the ternary germanides *RE*PdGe with the smaller rare earth elements.

Compound	Structure type	Space group	a (pm)	b (pm)	c (pm)	V (nm^3)	Reference
YPdGe	YbAuSn	*Imm*2	437.12(2)	2092.7(4)	756.5(2)	0.6920	This work
YPdGe	KHg_2 (subcell)	*Imma*	436.5(2)	695.2(3)	754.9(3)	0.2291	[1]
YPdGe	KHg_2 (subcell)	*Imma*	436.8	695.2	754.9	0.2292	[8]
LT-TbPdGe	YPdSi	*Pmmn*	438.9(9)	1398.2(3)	756.4(2)	0.4641	[21]
HT-TbPdGe	YbAuSn	*Imm*2	438.1(2)	2101.3(5)	757.4(2)	0.6972	This work
TbPdGe	KHg_2 (subcell)	*Imma*	438.1(1)	700.0(2)	757.3(3)	0.2322	[1]
TbPdGe	KHg_2 (subcell)	*Imma*	438.1	700.0	757.3	0.2322	[8]
TbPdGe	KHg_2 (subcell)	*Imma*	437.0(4)	696.1(7)	755.2(7)	0.2297	[15]
LT-DyPdGe	YPdSi	*Pmmn*	437.3(2)	1390.5(3)	754.8(2)	0.4590	This work
HT-DyPdGe	YbAuSn	*Imm*2	436.69(9)	2089.0(3)	755.93(9)	0.6896	This work
DyPdGe	KHg_2 (subcell)	*Imma*	436.6(2)	696.9(3)	755.6(3)	0.2299	[1]
DyPdGe	KHg_2 (subcell)	*Imma*	436.6	696.9	755.6	0.2299	[8]
DyPdGe	KHg_2 (subcell)	*Imma*	436.7(2)	693.7(2)	751.9(4)	0.2278	[19]
LT-HoPdGe	YPdSi	*Pmmn*	436.9(1)	1384.5(5)	754.6(2)	0.4564	This work
HT-HoPdGe	YbAuSn	*Imm*2	435.8(1)	2079.1(4)	755.1(2)	0.6842	This work
HoPdGe	KHg_2 (subcell)	*Imma*	436.0(2)	693.8(3)	754.7(3)	0.2283	[1]
HoPdGe	KHg_2 (subcell)	*Imma*	435.8	692.8	753.7	0.2276	[8]
HoPdGe	KHg_2 (subcell)	*Imma*	435.8(1)	692.2(4)	754.6(2)	0.2276	[13]
HoPdGe	KHg_2 (subcell)	*Imma*	436.6(2)	695.6(3)	759.6(4)	0.2307	[20]
HoPdGe	KHg_2 (subcell)	*Imma*	438.7(2)	697.7(3)	758.1(2)	0.2320	[19]
ErPdGe	YbAuSn	*Imm*2	435.0(1)	2066.6(3)	753.8(1)	0.6776	This work
ErPdGe	KHg_2 (subcell)	*Imma*	434.80(9)	690.0(2)	753.6(2)	0.2261	[1]
ErPdGe	KHg_2 (subcell)	*Imma*	434.8	690.0	753.6	0.2261	[8]
ErPdGe	KHg_2 (subcell)	*Imma*	431.4(2)	678.5(1)	742.3(3)	0.2173	[19]
TmPdGe	YbAuSn	*Imm*2	433.5(1)	2057.1(3)	753.2(1)	0.6717	This work
TmPdGe	KHg_2 (subcell)	*Imma*	433.8(1)	685.5(2)	752.4(2)	0.2237	[1]
TmPdGe	KHg_2 (subcell)	*Imma*	433.0	685.5	752.4	0.2233	[8]
YbPdGe	TiNiSi	*Pnma*	682.7(1)	432.8(1)	752.1(1)	0.2222	[7]
YbPdGe	KHg_2 (subcell)	*Imma*	434.4(3)	683.9(2)	752.2(3)	0.2235	[10]
YbPdGe	KHg_2 (subcell)	*Imma*	434.4	683.9	752.2	0.2235	[9]
YbPdGe	YbAuSn	*Imm*2	433.4(2)	2050.6(6)	752.6(2)	0.6689	[24]
LuPdGe	YbAuSn	*Imm*2	432.05(8)	2044.2(3)	752.5(2)	0.6646	This work

Experimental Section

Synthesis

Starting materials for the synthesis of the *RE*PdGe samples were ingots of the rare earth metals (Johnson Matthey or smart elements), palladium powder (Heraeus, *ca.* 200 mesh), and germanium lumps (Wacker), all with stated purities better than 99.9 %. Pieces of the rare earth ingots were first arc-melted [35] to small buttons under an argon atmosphere. The argon was purified before with molecular sieves, silica gel, and titanium sponge (900 K). Subsequently the rare earth buttons, cold-pressed pellets (∅ 6 mm) of palladium powder and pieces of the germanium lumps were weighed in the ideal 1 : 1 : 1 atomic ratios and reacted in the same arc-melting furnace. The product pellets were remelted three times to ensure homogeneity. The total weight losses after the various meltings were always smaller than 0.5 %. Pieces of the buttons were subsequently sealed in evacuated silica ampoules and annealed at 1070 K for two weeks in muffle furnaces. In the case of the dimorphic compounds, the high-temperature (HT) phases crystallized directly from the melt, and the low-temperature (LT) phases formed during the annealing procedures. The *RE*PdGe germanides are stable in air over years. Ground powders and polycrystalline samples are light grey, and single crystals have metallic lustre.

EDX data

Semiquantitative EDX analyses on the nine crystals investigated on the diffractometer were carried out by use of a Leica 420i scanning electron microscope with the rare earth trifluorides, palladium, and germanium as standards. The experimentally observed compositions were close to the ideal one. No impurity elements heavier than sodium (detection limit of the instrument) were found.

X-Ray diffraction

The polycrystalline samples (the as-cast and the annealed ones) were characterized by X-ray powder diffraction (Guinier technique, imaging plate detector, Fujifilm BAS-1800 readout system) using Cu$K_{\alpha 1}$ radiation and α-quartz (a = 491.30 and c = 540.46 pm) as an internal standard. The orthorhombic lattice parameters (Table 1) were refined from the powder data by a least-squares routine.

Table 2. Crystal data and structure refinement for *RE*PdGe (*RE* = Y, Tb, and Dy).

Compound	YPdGe	HT-TbPdGe	HT-DyPdGe	LT-DyPdGe
Structure type	YbAuSn	YbAuSn	YbAuSn	YPdSi
Space group; Z	*Imm*2; 12	*Imm*2; 12	*Imm*2; 12	*Pmmn*; 8
Lattice parameters	Table 1	Table 1	Table 1	Table 1
Molar mass, g mol^{-1}	267.90	337.91	341.49	341.49
Calculated density, g cm^{-3}	7.71	9.66	9.87	9.88
Absorption coefficient, mm^{-1}	45.2	50.2	52.4	52.5
Detector distance, mm	80	80	80	80
Exposure time, min	12	5	5	10
ω range; increment, deg	0 – 180, 1.0	0 – 180, 1.0	0 – 180, 1.0	0 – 180, 1.0
Integr. param. A, B, EMS	14.0; 2.4; 0.020	13.0; 2.3; 0.010	12.5; 2.0; 0.012	13.0; 3.0; 0.012
F(000), e	1404	1716	1728	1152
Crystal size, μm^3	$10 \times 30 \times 50$	$20 \times 50 \times 90$	$20 \times 30 \times 60$	$25 \times 40 \times 50$
Transm. ratio (max/min)	2.76	3.76	2.33	2.43
θ range, deg	2 – 32	2 – 32	2 – 32	2 – 32
Range in hkl	± 6, ± 30, ± 11	± 6, ± 31, ± 11	± 6, ± 30, ± 11	± 6, ± 20, ± 11
Total no. reflections	4062	4384	4202	3050
Independent reflections / $R_{\rm int}$	1301 / 0.063	1369 / 0.035	1337 / 0.068	916 / 0.034
Reflections with $I \geq 2\sigma(I)/R_\sigma$	496 / 0.124	896 / 0.032	534 / 0.093	374 / 0.053
Data / ref. parameters	1301 / 59	1369 / 59	1337 / 58	916 / 40
Goodness-of-fit on F^2	0.529	0.791	0.427	0.539
$R1/wR2$ for $I \geq 2\sigma(I)$	0.022 / 0.034	0.028 / 0.074	0.027 / 0.070	0.024 / 0.051
$R1/wR2$ for all data	0.077 / 0.039	0.039 / 0.071	0.076 / 0.090	0.057 / 0.056
Flack parameter	–	–	0.00(5)	–
BASF (twinning by inversion)	0.40(3)	0.29(3)	–	–
Extinction coefficient	0.00065(2)	0.00132(6)	0.0011(1)	0.00130(7)
Largest diff. peak /hole, e Å^{-3}	1.47 / −1.14	2.10 / −4.03	2.09 / −2.87	2.14 / −3.10

Table 3. Crystal data and structure refinement for *RE*PdGe (*RE* = Ho, Er, Tm, and Lu).

Compound	HT-HoPdGe	LT-HoPdGe	ErPdGe	TmPdGe	LuPdGe
Structure type	YbAuSn	YPdSi	YbAuSn	YbAuSn	YbAuSn
Space group; Z	*Imm*2; 12	*Pmmn*; 8	*Imm*2; 12	*Imm*2; 12	*Imm*2; 12
Lattice parameters	Table 1	Table 1	Table 1	Table 1	Table 1
Molar mass, g mol^{-1}	343.92	343.92	346.25	347.92	353.96
Calculated density, g cm^{-3}	10.02	10.01	10.18	10.32	10.61
Absorption coefficient, mm^{-1}	54.8	54.8	57.4	60.1	65.3
Detector distance, mm	80	80	80	80	80
Exposure time, min	15	10	10	12	20
ω range; increment, deg	0 – 180, 1.0	0 – 180, 1.0	0 – 180, 1.0	0 – 180, 1.0	0 – 180, 1.0
Integr. param. A, B, EMS	13.0; 3.0; 0.014	14.0; 2.1; 0.023	14.0; 2.4; 0.030	13.0; 3.0; 0.014	13.0; 3.0; 0.012
F(000), e	1740	1160	1752	1764	1788
Crystal size, μm^3	$20 \times 30 \times 80$	$20 \times 30 \times 70$	$30 \times 30 \times 100$	$50 \times 50 \times 80$	$50 \times 50 \times 80$
Transm. ratio (max/min)	6.60	4.82	2.69	2.19	2.50
θ range, deg	2 – 31	2 – 32	2 – 32	2 – 32	2 – 32
Range in hkl	± 6, ± 30, ± 10	± 6, ± 20, ± 11	± 6, ± 30, ± 11	± 6, ± 30, ± 11	± 6, ± 30, ± 11
Total no. reflections	4159	5330	4348	4304	3981
Independent reflections / $R_{\rm int}$	1260 / 0.052	906 / 0.050	1326 / 0.038	1321 / 0.033	1295 / 0.068
Reflections with $I \geq 2\sigma(I)/R_\sigma$	675 / 0.058	462 / 0.045	663 / 0.050	505 / 0.074	779 / 0.062
Data / ref. parameters	1260 / 59	906 / 40	1326 / 59	1321 / 59	1295 / 59
Goodness-of-fit on F^2	0.661	0.736	0.670	0.589	0.807
$R1/wR2$ for $I \geq 2\sigma(I)$	0.025 / 0.052	0.027 / 0.054	0.023 / 0.047	0.024 / 0.051	0.035 / 0.087
$R1/wR2$ for all data	0.048 / 0.056	0.064 / 0.060	0.048 / 0.050	0.063 / 0.054	0.057 / 0.093
BASF (twinning by inversion)	0.42(3)	–	0.36(3)	0.44(4)	0.15(4)
Extinction coefficient	0.00117(4)	0.0021(1)	0.00102(3)	0.00058(3)	0.0019(1)
Largest diff. peak /hole, e Å^{-3}	1.45 / −2.83	1.49 / −4.34	1.36 / −2.38	1.67 / −3.45	3.42 / −5.59

The correct indexing was ensured through intensity calculations [36] taking the atomic positions obtained from the structure refinements.

Irregularly-shaped single crystals of YPdGe, HT-TbPdGe, LT-DyPdGe, HT-DyPdGe, LT-HoPdGe, HT-HoPdGe, ErPdGe, TmPdGe, and LuPdGe were selected from the crushed

Table 4. Atomic coordinates and isotropic displacement parameters (pm^2) of YPdGe, TbPdGe, HT-DyPdGe, LT-DyPdGe, HT-HoPdGe, LT-HoPdGe, ErPdGe, TmPdGe, and LuPdGe. U_{eq} is defined as one third of the trace of the orthogonalized U_{ij} tensor.

Atom	Wyckoff site	*x*	*y*	*z*	U_{eq}
YPdGe (YbAuSn type)					
Y1	2*a*	0	0	0.5293(9)	69(12)
Y2	4*d*	0	0.3335(2)	0.5330(6)	91(9)
Y3	2*b*	0	1/2	0.4498(9)	59(12)
Y4	4*d*	0	0.1671(2)	0.4545(6)	72(9)
Pd1	4*d*	0	0.1044(2)	0.8290(5)	72(7)
Pd2	4*d*	0	0.2671(2)	0.1668(5)	105(7)
Pd3	4*d*	0	0.4282(2)	0.8221(5)	83(7)
Ge1	4*d*	0	0.0663(2)	0.1589(7)	60(9)
Ge2	4*d*	0	0.2338(3)	0.8404(9)	88(10)
Ge3	4*d*	0	0.4057(2)	0.1552(7)	56(10)
TbPdGe (YbAuSn type)					
Tb1	2*a*	0	0	0.46492(17)	72(3)
Tb2	4*d*	0	0.66614(5)	0.46470(10)	72(3)
Tb3	2*b*	0	1/2	0.54764(15)	53(3)
Tb4	4*d*	0	0.83282(5)	0.54125(11)	61(3)
Pd1	4*d*	0	0.89604(9)	0.1730(2)	76(4)
Pd2	4*d*	0	0.73368(11)	0.8345(2)	102(4)
Pd3	4*d*	0	0.57163(10)	0.1762(3)	63(4)
Ge1	4*d*	0	0.93519(13)	0.8451(2)	50(5)
Ge2	4*d*	0	0.76517(15)	0.1645(3)	76(6)
Ge3	4*d*	0	0.59421(15)	0.8450(3)	72(5)
HT-DyPdGe (YbAuSn type)					
Dy1	2*a*	0	0	0.4647(3)	58(6)
Dy2	4*d*	0	0.66653(9)	0.4649(2)	54(4)
Dy3	2*b*	0	1/2	0.5486(3)	61(6)
Dy4	4*d*	0	0.83273(9)	0.5412(2)	62(4)
Pd1	4*d*	0	0.89609(14)	0.1716(5)	55(7)
Pd2	4*d*	0	0.73329(19)	0.8341(5)	84(7)
Pd3	4*d*	0	0.57217(16)	0.1774(5)	67(7)
Ge1	4*d*	0	0.9348(2)	0.8440(6)	81(11)
Ge2	4*d*	0	0.7646(3)	0.1625(6)	58(10)
Ge3	4*d*	0	0.5943(3)	0.8453(6)	69(10)
LT-DyPdGe (YPdSi type)					
Dy1	4*e*	1/4	0.00122(5)	0.78635(8)	57(2)
Dy2	2*b*	1/4	3/4	0.71075(14)	62(2)
Dy3	2*a*	1/4	1/4	0.70429(13)	61(2)
Pd1	4*e*	1/4	0.14160(9)	0.07730(17)	69(3)
Pd2	4*e*	1/4	0.59610(9)	0.41814(17)	82(3)
Ge1	4*e*	1/4	0.10608(13)	0.4091(2)	66(4)
Ge2	4*e*	1/4	0.65223(12)	0.0902(2)	54(4)
HT-HoPdGe (YbAuSn type)					
Ho1	2*a*	0	0	0.5352(3)	55(5)
Ho2	4*d*	0	0.33350(8)	0.53527(15)	52(3)
Ho3	2*b*	0	1/2	0.4514(3)	60(5)
Ho4	4*d*	0	0.16694(9)	0.45904(18)	68(4)
Pd1	4*d*	0	0.10407(13)	0.8279(4)	61(6)
Pd2	4*d*	0	0.26726(18)	0.1668(5)	95(6)
Pd3	4*d*	0	0.42803(15)	0.8228(5)	58(6)
Ge1	4*d*	0	0.0655(2)	0.1538(5)	64(9)
Ge2	4*d*	0	0.2354(2)	0.8360(6)	73(8)
Ge3	4*d*	0	0.4062(2)	0.1541(5)	63(8)
LT-HoPdGe (YPdSi type)					
Ho1	4*e*	1/4	0.00105(5)	0.78607(8)	65(2)
Ho2	2*b*	1/4	3/4	0.7106(1)	76(2)
Ho3	2*a*	1/4	1/4	0.7038(1)	72(2)
Pd1	4*e*	1/4	0.14137(9)	0.0767(2)	70(2)
Pd2	4*e*	1/4	0.59545(9)	0.4186(2)	87(3)
Ge1	4*e*	1/4	0.1063(1)	0.4086(2)	78(3)
Ge2	4*e*	1/4	0.65219(12)	0.0911(2)	62(3)
ErPdGe (YbAuSn type)					
Er1	2*a*	0	0	0.5350(3)	57(5)
Er2	4*d*	0	0.33321(9)	0.53558(15)	60(4)
Er3	2*b*	0	1/2	0.4519(3)	58(6)
Er4	4*d*	0	0.16698(9)	0.45888(19)	71(4)
Pd1	4*d*	0	0.10439(15)	0.8272(4)	73(6)
Pd2	4*d*	0	0.26675(18)	0.1665(5)	91(7)
Pd3	4*d*	0	0.42849(15)	0.8220(5)	78(7)
Ge1	4*d*	0	0.0658(2)	0.1536(5)	49(10)
Ge2	4*d*	0	0.2356(2)	0.8363(6)	80(10)
Ge3	4*d*	0	0.4066(2)	0.1536(5)	48(8)
TmPdGe (YbAuSn type)					
Tm1	2*a*	0	0	0.4660(5)	68(9)
Tm2	4*d*	0	0.66708(13)	0.4631(2)	56(6)
Tm3	2*b*	0	1/2	0.5460(5)	78(9)
Tm4	4*d*	0	0.83323(13)	0.5424(3)	71(6)
Pd1	4*d*	0	0.8953(3)	0.1755(7)	71(10)
Pd2	4*d*	0	0.7328(3)	0.8362(6)	98(10)
Pd3	4*d*	0	0.5710(3)	0.1791(7)	95(12)
Ge1	4*d*	0	0.9334(3)	0.8453(9)	43(14)
Ge2	4*d*	0	0.7640(4)	0.1599(7)	66(15)
Ge3	4*d*	0	0.5935(4)	0.8445(9)	58(13)
LuPdGe (YbAuSn type)					
Lu1	2*a*	0	0	0.5338(3)	73(4)
Lu2	4*d*	0	0.33281(7)	0.53604(16)	67(3)
Lu3	2*b*	0	1/2	0.4520(3)	90(5)
Lu4	4*d*	0	0.16640(7)	0.45858(19)	91(3)
Pd1	4*d*	0	0.10462(14)	0.8272(4)	80(6)
Pd2	4*d*	0	0.26862(19)	0.1691(5)	122(7)
Pd3	4*d*	0	0.42770(16)	0.8220(4)	66(5)
Ge1	4*d*	0	0.0661(2)	0.1521(6)	80(9)
Ge2	4*d*	0	0.2370(3)	0.8386(6)	99(9)
Ge3	4*d*	0	0.4074(3)	0.1524(5)	82(8)

arc-melted or annealed samples. The quality of the crystals was first checked by Laue photographs on a Buerger camera (white Mo radiation). Intensity data were measured at r. t. by use of a Stoe IPDS-II imaging plate diffractometer in oscillation mode (graphite-monochromatized MoK_α radiation). Numerical absorption corrections were applied to the data sets. All relevant details concerning the data collections and evaluations are listed in Tables 2 and 3.

Structure refinements

As emphasized in the Introduction, seven superstructures of the orthorhombic KHg_2 type are known. Since the Guinier patterns of the as-cast and annealed samples of TbPdGe,

Table 5. Interatomic distances (pm) calculated with the powder lattice parameters of LT-DyPdGe and LuPdGe. All distances within the first coordination spheres are listed. Standard deviations are all equal or less than 0.5 pm.

LT-DyPdGe (YPdSi type)

Dy1:	1	Pd1	293.8	Dy3:	2	Ge1	299.5	Ge1:	2	Pd2	255.0
	2	Pd2	298.4		4	Ge2	300.6		1	Pd1	255.3
	2	Ge1	303.0		2	Pd1	319.4		1	Pd2	281.2
	1	Pd2	309.1		4	Pd2	319.6		1	Dy3	299.5
	2	Pd1	312.8		2	Dy1	351.4		2	Dy1	303.0
	1	Ge2	313.3		2	Dy2	382.0		2	Dy2	309.9
	2	Ge2	317.1	Pd1:	2	Ge2	253.0		1	Dy1	319.9
	1	Ge1	319.9		1	Ge1	255.3	Ge2:	2	Pd1	253.0
	1	Dy3	351.4		1	Dy1	293.8		1	Pd2	259.5
	1	Dy2	354.0		1	Pd1	301.5		1	Ge2	271.9
	2	Dy1	389.7		2	Dy2	310.0		2	Dy3	300.6
Dy2:	2	Pd2	307.5		2	Dy1	312.8		1	Dy1	313.3
	4	Ge1	309.9		1	Dy3	319.4		2	Dy1	317.1
	4	Pd1	310.0	Pd2:	2	Ge1	255.0		1	Dy2	317.1
	2	Ge2	317.1		1	Ge2	259.5				
	2	Dy1	354.0		1	Ge1	281.2				
	2	Dy3	382.0		2	Dy1	298.4				
					1	Dy2	307.5				
					1	Dy1	309.1				
					2	Dy3	319.6				

LuPdGe (YbAuSn type)

Lu1:	4	Ge3	300.8	Lu4:	2	Pd2	299.0	Pd3:	2	Ge1	251.4
	4	Pd3	306.5		2	Ge3	301.2		1	Ge3	252.1
	2	Pd1	307.4		1	Pd2	301.9		1	Lu2	289.7
	2	Ge1	317.4		1	Pd1	304.8		1	Pd3	295.6
	2	Lu4	344.8		2	Ge2	306.3		2	Lu1	306.5
	2	Lu3	381.7		2	Pd3	307.0		2	Lu4	307.0
Lu2:	1	Pd3	289.7		1	Ge1	308.7		1	Lu3	315.2
	2	Pd1	296.2		1	Ge2	320.3	Ge1:	2	Pd3	251.4
	2	Ge2	298.6		1	Lu1	344.8		1	Pd1	256.9
	1	Ge2	300.3		1	Lu2	345.1		1	Ge1	270.1
	1	Pd2	305.7		2	Lu2	384.4		2	Lu3	295.9
	2	Ge1	311.5	Pd1:	2	Ge3	254.1		1	Lu4	308.7
	2	Pd2	315.7		1	Ge1	256.9		2	Lu2	311.5
	1	Ge3	326.5		1	Ge2	270.8		1	Lu1	317.4
	1	Lu4	345.2		2	Lu2	296.2	Ge2:	2	Pd2	251.1
	1	Lu3	347.6		1	Lu4	304.8		1	Pd2	257.0
	2	Lu4	384.4		1	Lu1	307.4		1	Pd1	270.8
Lu3:	2	Ge3	294.4		2	Lu3	318.2		2	Lu2	298.6
	4	Ge1	295.9	Pd2:	2	Ge2	251.1		1	Lu2	300.3
	2	Pd3	315.2		1	Ge2	257.0		2	Lu4	306.3
	4	Pd1	318.2		1	Ge3	284.0		1	Lu4	320.3
	2	Lu2	347.6		2	Lu4	299.0	Ge3:	1	Pd3	252.1
	2	Lu1	381.7		1	Lu4	301.9		2	Pd1	254.1
					1	Lu2	305.7		1	Pd2	284.0
					2	Lu2	315.7		1	Lu3	294.4
									2	Lu1	300.8
									2	Lu4	301.2
									1	Lu2	326.5

DyPdGe, and HoPdGe gave already hints for different superstructures, all single crystal data sets obtained from the image plate diffractometers were carefully evaluated. The cell enlargement factor (1, 2, 3, or 5, *i. e.* multiples of the *b* axis of the KHg_2 subcell) and the type of the Bravais lattice (*P* or *I*) allowed for a clear assignment of the superstructure type. Accordingly, YPdGe, HT-TbPdGe, HT-DyPdGe, HT-HoPdGe, ErPdGe, TmPdGe, and LuPdGe crystallize with the non-centrosymmetric YbAuSn type [34], space group *Imm*2, while LT-DyPdGe and LT-HoPdGe adopt the YPdSi structure [31], space group *Pmmn*. The atomic sites of YbPdGe (*Imm*2) [24] and CePtGe (*Pmmn*) [37] were taken as starting parameters. The nine structures were refined using SHELXL-97 [38] (full-matrix least-squares on F^2) with anisotropic atomic displacement parameters for all atoms.

In order to check for the possibility of mixed Pd/Ge sites, the occupancy parameters were refined in separate series of least-squares cycles. Since all sites were fully occupied within two standard deviations, in the final cycles the ideal occupancy parameters were assumed again. Refinement of the correct absolute structure for the non-centrosymmetric YbAuSn-type germanides (space group *Imm*2) was ensured through calculation of the Flack parameters [39, 40]. Most crystals showed twinning by inversion. The final difference Fourier syntheses were flat (Tables 2 and 3). The positional parameters and interatomic distances (exemplarily for LT-DyPdGe and LuPdGe) are listed in Tables 4 and 5.

Further details of the crystal structure investigations may be obtained from Fachinformationszentrum Karlsruhe, 76344 Eggenstein-Leopoldshafen, Germany (fax: +49-7247-808-666; e-mail: crysdata@fiz-karlsruhe.de, http://www.fiz-informationsdienste.de/en/DB/icsd/depot_anforderung.html) on quoting the deposition numbers CSD-391466 (YPdGe), CSD-391465 (HT-TbPdGe), CSD-391464 (LT-DyPdGe), CSD-391463 (HT-DyPdGe), CSD-391462 (LT-HoPdGe), CSD-391461 (HT-HoPdGe), CSD-420247 (ErPdGe), CSD-420246 (TmPdGe), and CSD-420245 (LuPdGe).

Discussion

By the synthesis of the new germanide LuPdGe and the structure refinements of YPdGe, HT-TbPdGe, LT-DyPdGe, HT-DyPdGe, LT-HoPdGe, HT-HoPdGe, ErPdGe, and TmPdGe the crystal chemical data on the *RE*PdGe germanides have been completed. All previous studies on the orthorhombic *RE*PdGe germanides reported only the KHg_2-type subcell structures with a statistical distribution of the palladium and germanium atoms. Also a single crystal study of a crystal taken

type \ *RE*	Sc	Y	La	Ce	Pr	Nd	Pm	Sm	Eu	Gd	Tb	Dy	Ho	Er	Tm	Yb	Lu
ZrNiAl	×																
EuNiGe									×								
CaCuGe			×	×	×	×		×		LT							
YPdSi										HT	LT	LT	LT				
YbAuSn		×									HT	HT	HT	×	×	×	×

Fig. 1. Structure types for the *RE*PdGe germanides. LT and HT denote low- and high-temperature modifications.

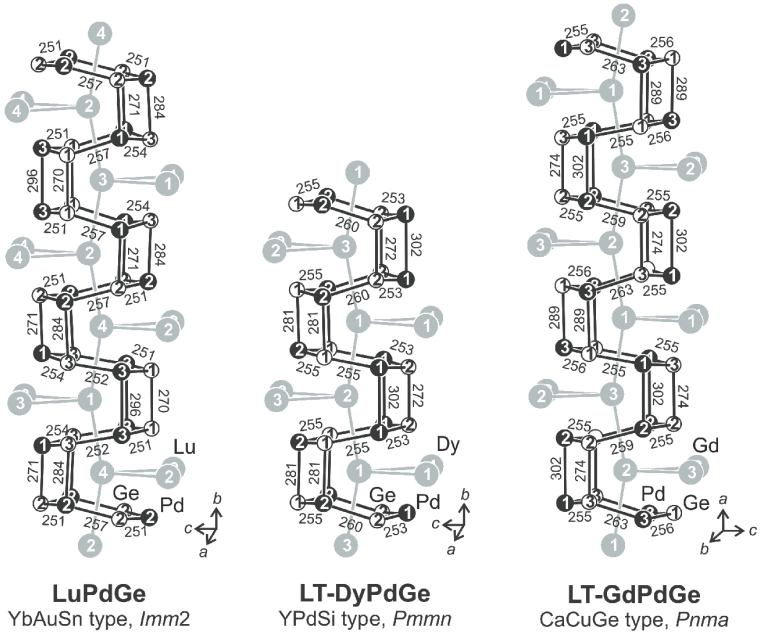

Fig. 2. Coordination of the rare earth atoms in the germanides LuPdGe, LT-DyPdGe, and LT-GdPdGe [21]. Relevant interatomic distances are given (pm). For details see text.

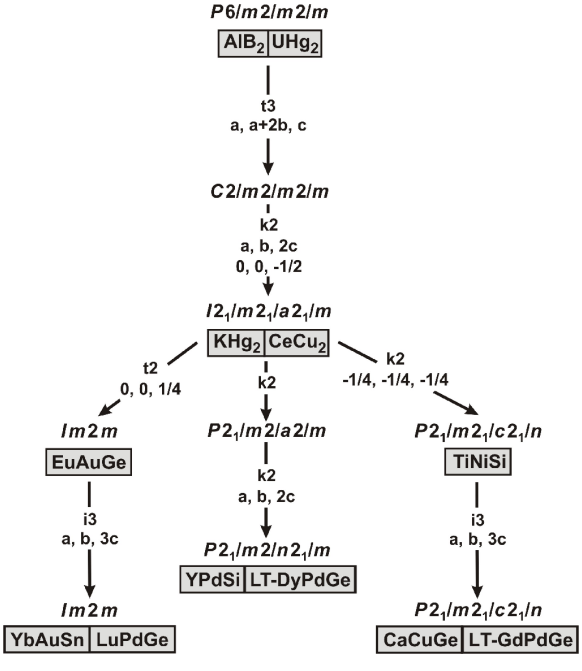

⟵ Fig. 3. Group-subgroup scheme in the Bärnighausen formalism [43 – 45] for the structures of LuPdGe, LT-DyPdGe, and LT-GdPdGe starting from the aristotype AlB_2 [27]. The indices for the *klassengleiche* (k), *isomorphic* (i), and *translationengleiche* (t) symmetry reductions as well as the unit cell transformations are given. Non-standard settings of several space groups have been used in order to keep the symmetry reductions simple. For details see text.

from a sample annealed at 870 K revealed the Pd/Ge statistics [20]. Most likely the weak superstructure reflections were overlooked in the previous work. Neutron powder diffraction studies on arc-melted samples annealed at 1070 K for 100 h of TbPdGe, DyPdGe, HoPdGe, and ErPdGe [15, 19] were all based on the KHg_2-type subcells with statistical Pd/Ge occupancy on the 8*h* sites in space group *Imma*. In view of the wrong assignment of the nuclear structures, the proposed models for the magnetic structures are questionable. The magnetic symmetry group of the germanide in the magnetically ordered state should be a subgroup of the magnetic group in the paramagnetic regime [41, 42].

As emphasized in Fig. 1, all orthorhombic *RE*PdGe germanides show full Pd/Ge ordering. With *RE* = La, Ce, Pr, Nd, and Sm the YPdSi-type [31] structure, space group *Pmmn*, occurs, while the germanides with the smaller rare earth elements Y and Er–Lu adopt an YbAuSn-type [34] ordering, space group *Imm*2. The compounds with Gd, Tb, Dy, and Ho are dimorphic with completely ordered Pd_3Ge_3 hexagons in the low- and high-temperature modifications. The cell volumes per formula unit *RE*PdGe decrease from the lanthanum to the lutetium compound as expected from the lanthanoid contraction. The cell volume of YPdGe is close

to that observed for HoPdGe. YPdGe and the *RE*PdGe germanides with the smaller rare earth elements show no dimorphism.

Exemplarily for each ordering variant we present the near-neighbor coordination of the rare earth atoms in LT-GdPdGe (CaCuGe type, space group *Pnma* [21]), LT-DyPdGe (YPdSi type, space group *Pmmn*) and the new germanide LuPdGe (YbAuSn type, space group *Imm*2) in Fig. 2. The three ordering variants are derived from the aristotype AlB_2 *via* group-subgroup relations [43 – 45] (Fig. 3). The common structural motifs of the three structures are slightly puckered, ordered Pd_3Ge_3 hexagons with intra-layer Pd–Ge distances ranging from 252 to 263 pm. As a function of the rare earth element size (lanthanoid contraction) these distances decrease slightly from LT-GdPdGe to LuPdGe. They are all close to the sum of the covalent radii [46] of 250 pm, indicating substantial covalent Pd–Ge bonding within these networks.

The orientation of the differently stacked Pd_3Ge_3 hexagons in the three different superstructures leads to rather short Pd–Ge interlayer distances (271 – 289 pm), and also Pd–Pd (296 – 302 pm) and Ge–Ge contacts (270 – 274 pm) indicating weak interactions. The latter are longer than in *fcc* palladium (275 pm) and elemental germanium (245 pm) [47]. The Pd–Pd interactions might be the driving force for superstructure formation. Similar to many dinuclear palladium complexes [48], we can expect closed-shell d^{10}-d^{10} interactions, well known for silver [49] and gold [50, 51] compounds. The kind of superstructure formed for a given *RE*PdGe germanide at a given temperature seems to be the result of a complex interplay of geometric (lanthanoid contraction) and electronic factors as well. Prediction of the superstructure variant is not possible as yet.

Acknowledgement

This work was financially supported by the Deutsche Forschungsgemeinschaft.

[1] E. Hovestreydt, N. Engel, K. Klepp, B. Chabot, E. Parthé, *J. Less-Common Met.* **1982**, *85*, 247.
[2] E. Hovestreydt, *J. Less-Common Met.* **1988**, *143*, 25.
[3] P. Rogl, B. Chevalier, M. J. Besnus, J. Etourneau, *J. Magn. Magn. Mater.* **1989**, *80*, 305.
[4] B. Chevalier, P. Rogl, J. Etourneau, M. J. Besnus, *J. Magn. Magn. Mater.* **1990**, *83*, 303.
[5] J. Sakurai, Y. Yamaguchi, S. Nishigori, T. Suzuki, T. Fujita, *J. Magn. Magn. Mater.* **1990**, *90 & 91*, 422.
[6] M. J. Besnus, A. Braghta, N. Hamdaoui, A. Meyer, *J. Magn. Magn. Mater.* **1992**, *104 – 107*, 1385.
[7] B. Sendlinger, Dissertation, Ludwig-Maximilians-Universität München, München, **1993**.
[8] P. A. Kotsanidis, J. K. Yakinthos, E. Roudaut, H. Gamari-Seale, *J. Magn. Magn. Mater.* **1994**, *131*, 139.
[9] V. N. Nikiforov, M. V. Kovachikova, A. A. Velikhovskii, Yu. V. Kochetkov, J. Mircovic, O. M. Borisenko, Yu. D. Seropegin, *Fiz. Tver. Tela* **1994**, *36*, 471.
[10] Yu. D. Seropegin, O. L. Borisenko, O. I. Bodak, V. N. Nikiforov, M. V. Kovachikova, Yu. V. Kochetkov, *J. Alloys Compd.* **1994**, *216*, 259.
[11] R. Pöttgen, *Z. Naturforsch.* **1995**, *50b*, 1181.
[12] A. V. Morozkin, Yu. D. Seropegin, *J. Alloys Compd.* **1996**, *237*, 124.
[13] O. Sologub, K. Hiebl, P. Rogl, H. Noël, *J. Alloys Compd.* **1996**, *245*, L13.
[14] Zh. M. Barakatova, Yu. D. Seropegin, O. I. Bodak, B. D. Belan, *Inorg. Mater.* **1996**, *32*, 581.
[15] A. Szytuła, M. Kolenda, E. Ressouche, A. Zygmunt, *J. Alloys Compd.* **1997**, *259*, 36.
[16] Zh. M. Kurenbaeva, Yu. D. Seropegin, O. I. Bodak, V. N. Nikiforov, *J. Alloys Compd.* **1998**, *269*, 151.
[17] Yu. D. Seropegin, A. V. Gribanov, O. I. Bodak, *J. Alloys Compd.* **1998**, *269*, 157.
[18] Y. Itoh, H. Kadomatsu, *J. Alloys Compd.* **1998**, *280*, 39.
[19] B. Penc, M. Hofmann, A. Szytuła, A. Zygmunt, *J. Alloys Compd.* **1999**, *282*, 52.
[20] O. L. Sologub, P. S. Salamakha, *J. Alloys Compd.* **1999**, *291*, 181.
[21] D. Niepmann, Yu. M. Prots', R. Pöttgen, W. Jeitschko, *J. Solid State Chem.* **2000**, *154*, 329.
[22] X. Rocquefelte, R. Gautier, J.-F. Halet, R. Müllmann, C. Rosenhahn, B. D. Mosel, G. Kotzyba, R. Pöttgen, *J. Solid State Chem.* **2007**, *180*, 533.
[23] W. Hermes, U. Ch. Rodewald, B. Chevalier, R. Pöttgen, *Z. Naturforsch.* **2007**, *62b*, 613.
[24] K. Katoh, B. Heying, R.-D. Hoffmann, U. Ch. Rodewald, R. Pöttgen, *Z. Anorg. Allg. Chem.* **2008**, *634*, 1296.
[25] E. J. Duwell, N. C. Baenziger, *Acta Crystallogr.* **1955**, *8*, 705.
[26] A. C. Larson, D. T. Cromer, *Acta Crystallogr.* **1961**, *14*, 73.
[27] R.-D. Hoffmann, R. Pöttgen, *Z. Kristallogr.* **2001**, *216*, 127.
[28] C. B. Shoemaker, D. P. Shoemaker, *Acta Crystallogr.* **1965**, *18*, 900.

[29] W. Dörrscheidt, N. Niess, H. Schäfer, *Z. Naturforsch.* **1977**, *32b*, 985.
[30] D. Kußmann, R.-D. Hoffmann, R. Pöttgen, *Z. Anorg. Allg. Chem.* **1998**, *624*, 1727.
[31] Yu. M. Prots', R. Pöttgen, W. Jeitschko, *Z. Anorg. Allg. Chem.* **1998**, *624*, 425.
[32] R. Pöttgen, *J. Mater. Chem.* **1995**, *5*, 505.
[33] R. Pöttgen, R.-D. Hoffmann, R. Müllmann, B. D. Mosel, G. Kotzyba, *Chem. Eur. J.* **1997**, *3*, 1852.
[34] R.-D. Hoffmann, R. Pöttgen, D. Kußmann, R. Müllmann, B. D. Mosel, *Chem. Mater.* **2001**, *13*, 4019.
[35] R. Pöttgen, Th. Gulden, A. Simon, *GIT Labor-Fachzeitschrift* **1999**, *43*, 133.
[36] K. Yvon, W. Jeitschko, E. Parthé, *J. Appl. Crystallogr.* **1977**, *10*, 73.
[37] Yu. M. Prots', R. Pöttgen, D. Niepmann, M. W. Wolff, W. Jeitschko, *J. Solid State Chem.* **1999**, *142*, 400.
[38] G. M. Sheldrick, SHELXL-97, Program for the Refinement of Crystal Structures, University of Göttingen, Göttingen (Germany) **1997**.
[39] H. D. Flack, G. Bernadinelli, *Acta Crystallogr.* **1999**, *A55*, 908.
[40] H. D. Flack, G. Bernadinelli, *J. Appl. Crystallogr.* **2000**, *33*, 1143.
[41] A. P. Cracknell, J. Lorenc, J. A. Przystawa, *J. Phys. C: Solid State Phys.* **1976**, *9*, 1731.
[42] A. Authier (Ed.), *International Tables for Crystallography*, Vol. D, *Physical Properties of Crystals*, The International Union of Crystallography, Kluwer Academic Publishers, **2003**, Section 1.5.2., pp. 109 – 116.
[43] H. Bärnighausen, *Commun. Math. Chem.* **1980**, *9*, 139.
[44] H. Bärnighausen, U. Müller, *Symmetriebeziehungen zwischen den Raumgruppen als Hilfsmittel zur straffen Darstellung von Strukturzusammenhängen in der Kristallchemie*, University of Karlsruhe, Karlsruhe, University/GH Kassel, Kassel, **1996**.
[45] U. Müller, *Z. Anorg. Allg. Chem.* **2004**, *630*, 1519.
[46] J. Emsley, *The Elements*, Oxford University Press, Oxford, **1999**.
[47] J. Donohue, *The Structures of the Elements*, Wiley, New York, **1974**.
[48] T. Murahashi, H. Kurosawa, *Coord. Chem. Rev.* **2002**, *231*, 207.
[49] M. Jansen, *Angew. Chem.* **1987**, *99*, 1136; *Angew. Chem., Int. Ed. Engl.* **1987**, *26*, 1098.
[50] P. Pyykkö, N. Runeberg, F. Mendizabal, *Chem. Eur. J.* **1997**, *3*, 1451.
[51] H. Schmidbaur, A. Schier, *Chem. Soc. Rev.* **2008**, 1931.